PCP
PLANT & CELL PHYSIOLOGY

Vacuolar Protein Degradation via Autophagy Provides Substrates to Amino Acid Catabolic Pathways as an Adaptive Response to Sugar Starvation in *Arabidopsis thaliana*

Takaaki Hirota[1,5], Masanori Izumi[2,3,4,5], Shinya Wada[1,6], Amane Makino[1] and Hiroyuki Ishida[1,*]

[1]Department of Applied Plant Science, Graduate School of Agricultural Science, Tohoku University, Aramaki Aza Aoba, Sendai, 980-8572 Japan
[2]Frontier Research Institute for Interdisciplinary Sciences, Tohoku University, Aramaki Aza Aoba, Sendai, 980-8578 Japan
[3]Department of Environmental Life Sciences, Graduate School of Life Sciences, Tohoku University, Katahira, Sendai, 980-8577 Japan
[4]PRESTO, Japan Science and Technology Agency, Kawaguchi, 332-0012 Japan
[5]These authors contributed equally to this work
[6]Present address: Faculty of Agriculture, Iwate University, 3-18-8 Ueda, Morioka, Iwate, 020-8550 Japan
*Corresponding author: E-mail, hiroyuki@tohoku.ac.jp; Fax, +81-22-757-4289
(Received September 22, 2017; Accepted January 4, 2018)

The vacuolar lytic degradation of proteins releases free amino acids that plants can use instead of sugars for respiratory energy production. Autophagy is a major cellular process leading to the transport of proteins into the vacuole for degradation. Here, we examine the contribution of autophagy to the amino acid metabolism response to sugar starvation in mature leaves of *Arabidopsis thaliana*. During sugar starvation arising from the exposure of wild-type (WT) plants to darkness, autophagic transport of chloroplast stroma, which contains most of the proteins in a leaf, into the vacuolar lumen was induced within 2 d. During this time, the level of soluble proteins, primarily Rubisco (ribulose-1,5-bisphosphate carboxylase/oxygenase), decreased and the amount of free amino acid increased. In dark-treated autophagy-defective (*atg*) mutants, the decrease of soluble proteins was suppressed, which resulted in the compromised release of basic amino acids, branched-chain amino acids (BCAAs) and aromatic amino acids. The impairment of BCAA catabolic pathways in the knockout mutants of the electron transfer flavoprotein (ETF)/ETF:ubiquinone oxidoreductase (*etfqo*) complex and the electron donor protein isovaleryl-CoA dehydrogenase (*ivdh*) caused a reduced tolerance to dark treatment similar to that in the *atg* mutants. The enhanced accumulation of BCAAs in the *ivdh* and *etfqo* mutants during the dark treatment was reduced by additional autophagy deficiency. These results indicate that vacuolar protein degradation via autophagy serves as an adaptive response to disrupted photosynthesis by providing substrates to amino acid catabolic pathways, including BCAA catabolism mediated by IVDH and ETFQO.

Keywords: Amino acid catabolism • Arabidopsis • Autophagy • Chloroplasts • Sugar starvation • Vacuolar protein degradation.

Abbreviations: *ATG*, *autophagy-related*; BCAA, branched-chain amino acid; D2HGDH, 2-hydroxyglutarate dehydrogenase; ETF, electron transfer flavoprotein; ETFQO, electron transfer flavoprotein:ubiquinone oxidoreductase; GFP, green fluorescent protein; IDH, isocitrate dehydrogenase; IVDH, isovaleryl-CoA dehydrogenase; qRT–PCR, quantitative reverse transcription–PCR; RCB, ribulose-1,5-bisphosphate carboxylase/oxygenase-containing body; RFP, red fluorescent protein; Rubisco, ribulose-1,5-bisphosphate carboxylase/oxygenase; TCA, tricarboxylic acid; WT, wild type.

Introduction

The vacuole is an organelle that occupies as much as >90% of the total volume of many types of mature plant cells. Its lytic activity arises from the various types of hydrolases it contains (Matile 1987). Vacuolar digestion of cytoplasmic macromolecules facilitates the reutilization of the released components, such as amino acids, lipids or nucleotides (Muntz 2007). This recycling of assimilated carbon or minerals is an important system that enables sessile land plants to survive and grow under naturally variable conditions in which the available energy and nutrients may be limited.

In land plants, the leaves require nutrients to enable the photosynthetic assimilation of atmospheric carbon dioxide (Makino et al. 1997). Assimilated carbohydrates become the major substrate for energy conversion via glycolysis and subsequent oxidative respiration. The availability of solar energy, which is necessary for photosynthesis, fluctuates in response to the climate or shading by other plants, while other suboptimal conditions, such as flooding, drought and extreme temperatures, can interfere with photosynthesis or respiration, perturbing the amount of energy a plant can harness (Baena-González and Sheen 2008). To survive under conditions with low energy availability, plants need an alternative to assimilated carbohydrates for energy production.

Exposing whole plants to darkness is widely used as an experimental model of low-energy stress, and was previously used to reveal that amino acids can serve as alternative substrates for respiratory energy production via the catabolic pathway (Araújo et al. 2011, Hildebrandt et al. 2015). Isovaleryl-CoA dehydrogenase (IVDH) and 2-hydroxyglutarate dehydrogenase

Plant Cell Physiol. 59(7): 1363–1376 (2018) doi:10.1093/pcp/pcy005, Advance Access publication on 30 January 2018, available online at www.pcp.oxfordjournals.org

(D2HGDH) were identified as enzymes facilitating the dark-induced catabolism of branched-chain amino acids (BCAAs) and lysine (Lys; Araújo et al. 2010). The reactions catalyzed by these enzymes release electrons, which are donated to the mitochondrial electron transfer flavoprotein (ETF)/ETF:ubiquinone oxidoreductase (ETFQO) complex, and are eventually transferred to ubiquinone pools to support respiration (Ishizaki et al. 2005, Ishizaki et al. 2006). Recent studies demonstrated an important role for the catabolism of BCAAs and Lys in plant survival under sugar starvation caused by darkness (Araújo et al. 2011, Schertl and Braun 2014, Hildebrandt et al. 2015).

Autophagy is an evolutionarily conserved system facilitating vacuolar protein degradation in eukaryotic cells. It is best understood in nutrient starvation conditions, when components such as proteins and organelles are sequestered by autophagosomes, transported into the vacuole, degraded by resident hydrolases and recycled. *Autophagy-related* (*ATG*) genes, which are essential for autophagy progression, were originally identified in yeast (Tsukada and Ohsumi 1993). To date, 41 *ATG* genes have been identified in yeast (Yao et al. 2015), 15 of which (*ATG1–ATG10*, *ATG12–ATG14*, *ATG16* and *ATG18*) are referred to as 'core' *ATG* genes (Nakatogawa et al. 2009), involved in the core machinery for autophagosomal membrane formation, and are essential for any type of autophagy. Orthologs of the yeast core *ATG* genes are also found in plant species, where they serve similar functions (Liu and Bassham 2012, Yoshimoto 2012).

There is growing evidence to support the importance of autophagy under sugar starvation conditions in plants, as it functions in other eukaryotes. Although the Arabidopsis mutants of the core *ATG* genes can complete their life cycles, they cannot survive long periods of darkness (Thompson et al. 2005). Additional mutations causing a starchless phenotype in *atg* plants, in which the major respiration source (starch) is not synthesized, led to reduced growth and leaf cell death symptoms (Izumi et al. 2013). A recent metabolomic analysis demonstrated the importance of autophagy in the early growth of Arabidopsis seedlings germinated in darkness, as the *atg* mutants had reduced levels of free amino acids (Avin-Wittenberg et al. 2015).

The photosynthetic carbon-fixing enzyme Rubisco (ribulose-1,5-bisphosphate carboxylase/oxygenase) is exceptionally abundant, accounting for approximately 50% of soluble leaf protein in C_3 species (Evans 1989); therefore, chloroplast proteins represent the most abundant nutrient resources for recycling. Our previous studies revealed that chloroplasts are transported to the vacuole for degradation by autophagy in two distinct processes; one via a specific type of autophagic body for stromal proteins [originally referred to as Rubisco-containing bodies (RCBs)] and the other as whole organelles (Ishida et al. 2014). RCBs are small vesicles around 1 μm in diameter, which provide piecemeal transport of the chloroplast stroma into the vacuole without the digestion of entire chloroplasts (Ishida et al. 2008). This RCB pathway is strongly activated in sugar-starved leaves (Izumi et al. 2010), and these previous findings suggest that the RCB pathway could promote efficient amino acid recycling via the vacuolar degradation of stromal proteins under sugar-starved conditions.

There is good evidence that autophagy and amino acid catabolism are important in the plant response to sugar starvation; however, the relationship between the autophagic degradation of chloroplast proteins in the vacuole and the subsequent utilization of the released free amino acids is not fully understood. In this study, we examine the physiological contribution of autophagy to amino acid catabolism activated by sugar starvation in Arabidopsis mature leaves.

Results

Sugar starvation occurs following the exposure of whole plants to darkness

We first confirmed that Arabidopsis plants suffered sugar starvation under our experimental dark treatment system. We cultivated wild-type (WT) Arabidopsis and the autophagy-defective mutant *atg5-1* for 18 d under long-day conditions, then grew them in darkness for several days and checked their major carbohydrate contents (**Fig. 1**). The levels of starch and sucrose (Suc) were similar between the WT and *atg5-1* before the dark treatment, and were comparably depleted after the 2 d dark treatment (**Fig. 1A**). Glucose (Glc) and fructose (Fru) levels were <1/20th of the Suc level before the dark treatment (day 0) and those levels were similar between the WT and *atg5-1* throughout the treatment (data not shown). These results indicated that autophagy deficiency did not affect the carbohydrate depletion during the dark treatment.

Several previous studies have established marker genes for sugar starvation, including *DARK-INDUCIBLE GENE 6* (*DIN6*), which encodes the glutamine-dependent ASPARAGINE SYNTHETASE (ASN1), and *ARABIDOPSIS TÓXICOS EN LEVADURA 8* (*ATL8*), which encodes a ubiquitin E3 ligase (Fujiki et al. 2001, Baena-González et al. 2007, Graf et al. 2010, Izumi et al. 2013). Transcripts of both these genes were strongly up-regulated in the WT and *atg5-1* plants during the dark treatment (**Fig. 1B**), which further demonstrates that the sugar starvation response occurred in the leaves of dark-grown plants.

We further attempted to monitor the status of the leaf mesophyll cells containing chloroplasts during the dark treatment. To this end, we generated transgenic plants expressing green fluorescent protein (GFP) under the control of the *DIN6* promoter (*ProDIN6:GFP*; **Fig. 1C**), and placed 18-day-old *ProDIN6:GFP* plants in darkness for up to 48 h. GFP signals were rarely observed in leaf mesophyll cells before the dark treatment (0 h), but began to appear after 12 h of darkness and increased in a time-dependent manner for the 48 h treatment in both the WT and *atg5-1* backgrounds (**Fig. 1D**). These results confirm that the response to sugar starvation occurs in mesophyll cells within 2 d of the dark treatment, which is hereafter defined as the early period of sugar starvation.

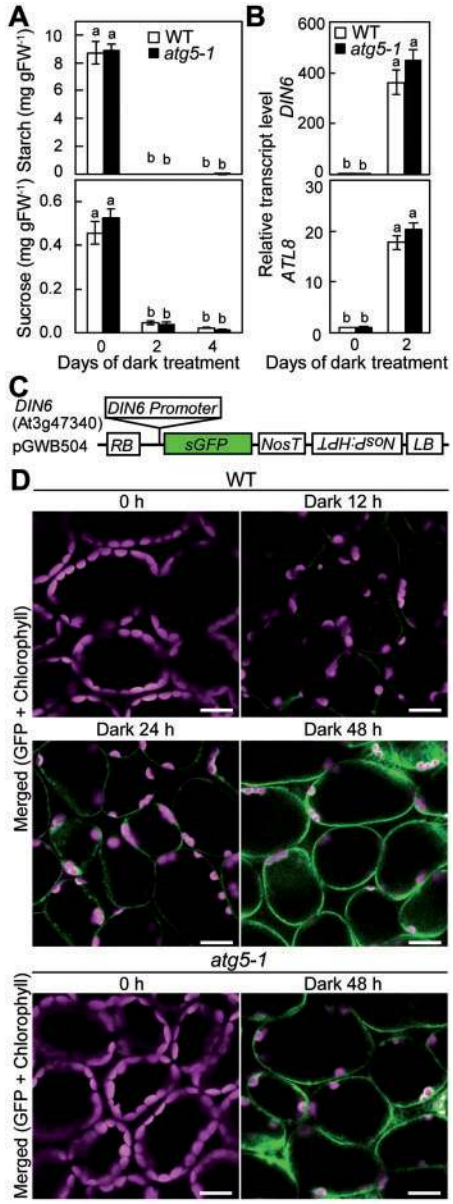

Fig. 1 Sugar starvation response caused by dark treatment. (A) The carbohydrate contents in wild-type (WT) and *atg5-1* leaves at 0 (at the end of the 18th day after sowing), 2 and 4 d after dark treatment. Data are means ± SE (n = 3). (B) The transcript levels of sugar starvation marker genes (*DIN6* and *ATL8*) at 0 and 2 d after dark treatment. Data are means ± SE (n = 3–4). Different letters denote significant differences from each other based on a Tukey test ($P \leq 0.05$). (C) A schematic representation of the *ProDIN6:GFP* construct. The promoter region of *DIN6* was cloned into pGWB504. HPT, hygromycin phosphotransferase; LB, left border; NosP and NosT, promoter and terminator sequences of the nopaline synthase gene; RB, right border; sGFP, synthetic GFP with the S65T mutation. (D) Visualization of the status of sugar starvation by expressing *GFP* under the control of the *DIN6* promoter. *ProDIN6:GFP* transgenic plants were grown in darkness for the indicated times, and leaves were observed using confocal laser-scanning microscopy. GFP fluorescence appears green and Chl autofluorescence appears magenta; merged images are shown. Scale bars = 20 μm.

Vacuolar degradation of chloroplast proteins via autophagy is activated from the early period of sugar starvation

We next investigated whether autophagy is activated in the leaf mesophyll cells from the early period of sugar starvation. Most leaf proteins are contained in the chloroplast stroma (Evans 1989), and autophagy of stromal proteins has been successfully monitored using transgenic plants expressing RBCS2B–fluorescent protein [GFP or red fluorescent protein (RFP)] fusions that assemble into the Rubisco holoenzyme with RbcL and RBCS to form Rubisco–GFP or Rubisco–RFP (Ishida et al. 2008, Ono et al. 2013). We therefore used this technique to examine the progression of chloroplast stroma-targeted autophagy via RCBs (**Fig. 2**). In *RBCS2B–RFP*-expressing plants, the Rubisco–RFP signal specifically labeled chloroplasts that exhibit a Chl signal under normal conditions (**Fig. 2A**). When these plants in the WT background were grown in darkness for 2 d, faint RFP signals appeared throughout the vacuolar lumen, while a few RFP-labeled RCBs appeared to move randomly (**Fig. 2A** arrowheads; Supplementary Movie S1). In contrast, RFP signals and RCBs were not observed in the vacuolar lumen of another *ATG5*-knockout mutant, *atg5-4*, expressing *RBCS2B–RFP* (**Fig. 2A**). Consistent with these observations, the intensity of vacuolar RFP was elevated in the dark-treated *RBCS2B–RFP* plants in the WT background, but not those in the *atg5* background (**Fig. 2A**).

Our previous studies also established a biochemical method to evaluate the occurrence of Rubisco autophagy by detecting the release of free GFP from the Rubisco–GFP fusion, which is specifically processed in the vacuole (Ono et al. 2013, Izumi et al. 2015). When soluble protein extract was subjected to non-denaturing PAGE followed by GFP fluorescence detection, the free GFP was found to appear after 2 d of dark treatment in *RBCS2B–GFP*-expressing plants with a WT background (**Fig. 2B**). In contrast, free-GFP was not observed in those with the *atg5-4* background even under prolonged darkness (up to 6 d; **Fig. 2B**). Similar results were consistently obtained in repeated experiments using individual plants. These results demonstrate that the autophagic transport of stromal proteins into the vacuolar lumen via the RCBs and their subsequent degradation is activated during the early period of sugar starvation.

We also monitored the behavior of the mitochondria under the dark treatment by labeling an enzyme of the mitochondrial tricarboxylic acid (TCA) cycle, isocitrate dehydrogenase (IDH), with GFP (IDH–GFP). There was no apparent difference in mitochondria between the control and dark conditions, or between plants with the WT and *atg5-4* backgrounds (Supplementary Fig. S1). No diffuse GFP signals were observed in the vacuolar lumens of dark-treated IDH–GFP plants (Supplementary Fig. S1).

Autophagy deficiency suppresses the decreases in Rubisco and soluble protein contents during the early period of sugar starvation

We further confirmed that the vacuolar accumulation of the RFP signal does not occur in Rubisco–RFP-expressing plants

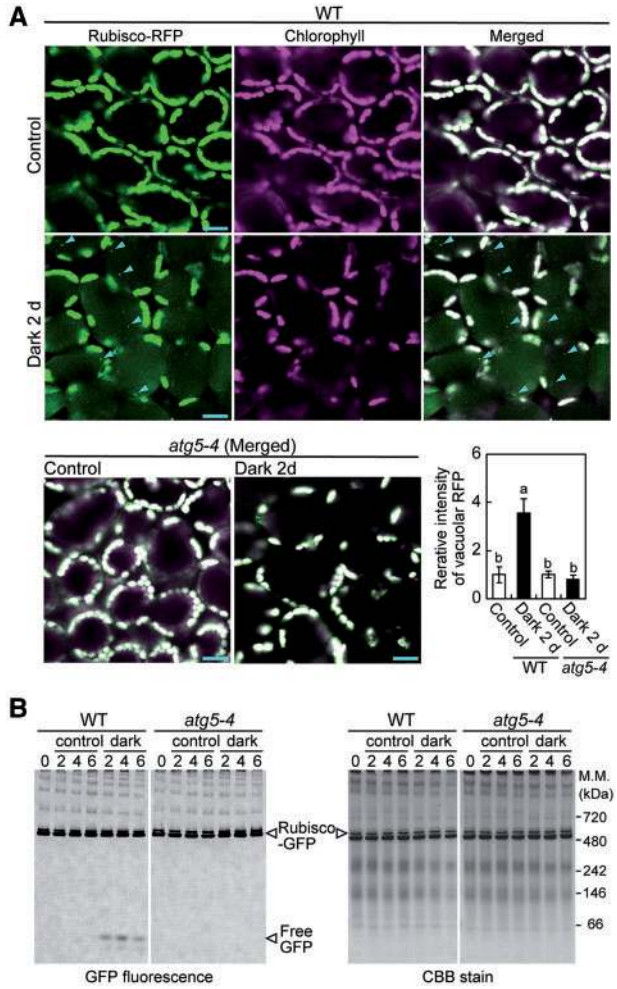

Fig. 2 Monitoring of Rubisco autophagy by examining fluorescent protein-labeled Rubisco. (A) Autophagic transport of Rubisco–RFP to the vacuolar lumen under dark treatment. RBCS2B–RFP-expressing plants in the WT or *atg5-4* background were grown in darkness for 2 d, and leaves were observed by confocal laser-scanning microscopy. RFP fluorescence appears green and Chl autofluorescence appears magenta. In the merged images, the overlap of GFP and Chl fluorescence appears white. Only merged images are shown for *atg5-4* plants. Blue arrowheads indicate Rubisco-containing bodies (RCBs). Scale bars = 20 μm. A bar graph shows average fluorescence intensity of RFP in the vacuolar lumen. Data are means ± SE (n = 10 cells). Different letters denote significant differences from each other based on a Tukey test ($P \leq 0.05$). (B) Autophagy-dependent processing of Rubisco–GFP under dark treatment. RBCS2B–GFP-expressing plants in the WT or *atg5-4* background were grown in darkness for the indicated period (0–6 d). Total soluble proteins were extracted from equal volumes of leaves and separated by non-denaturing PAGE, then either stained with Coomassie brilliant blue R250 or observed with a fluorescence image analyzer to detect GFP fluorescence.

with the background of *atg5-1* and the *ATG2*-knockout mutant (*atg2-1*) following 2 d of dark treatment (Supplementary Fig. S2). We assessed the impact of impaired autophagy in *atg5-1*, *atg5-4* and *atg2-1* on the dark stress-induced changes in the amounts of chloroplast components, including stromal proteins, by measuring the levels of Rubisco, soluble protein and Chl during an 8 d dark treatment of whole plants (**Fig. 3**). In WT plants, Rubisco levels decreased following 2 d of dark treatment (**Fig. 3A**), consistent with the observed activation of Rubisco autophagy (**Fig. 2**). In contrast, in *atg* plants, Rubisco levels did not decrease following 2 and 4 d of dark treatment, but rapidly decreased after longer periods of dark treatment, with a significant decrease observed at 8 d of dark treatment (**Fig. 3A**). We calculated and compared the proportional decrease in Rubisco levels, which clearly showed that the decrease of Rubisco is suppressed in *atg* plants during the early period of dark treatment, but not after 8 d of dark treatment (**Fig. 3B**). The changes in soluble protein levels were similar to those of Rubisco (**Fig. 3A, C**). These results support the notion that the degradation of soluble proteins, especially Rubisco, during the early period of sugar starvation is mainly caused by autophagy.

Although Chl levels decreased during the dark treatment in all genotypes (**Fig. 3A**), *atg* plants showed greater declines at the later periods of dark treatment (**Fig. 3A;** Supplementary Fig. S3). This result is consistent with the previously reported visibly enhanced chlorosis in the *atg* mutants under dark treatment (Hanaoka et al. 2002, Thompson et al. 2005, Phillips et al. 2008).

Dark-induced increases of total amino acid levels are suppressed in *atg* mutants

Several studies reported that free amino acid levels increase during the dark treatment of whole plants because proteins, which constitute reservoirs of amino acids, are actively degraded (Soudry et al. 2005, Araújo et al. 2010, Hildebrandt et al. 2015). We expected that the observed impairment of vacuolar protein degradation in the *atg* mutants affects the supply of free amino acids during sugar starvation; therefore, we measured the amino acid levels after 0, 2 and 4 d of dark treatment in the WT and the *atg* mutants (**Fig. 4**). We used the knockout mutant *atg10-1* as an additional mutant line of core *ATG* genes alongside *atg5-1* and *atg2-1*. Although the total amino acid levels increased during the dark treatment regardless of genotype (**Fig. 4A**), in the early periods of the dark treatment (0–2 d), the increase in total amino acid levels was suppressed in the *atg* mutants compared with the WT (**Fig. 4B**). These changes correspond to the limited decreases in Rubisco and soluble proteins observed in the *atg* plants within the 2 d dark treatment (**Fig. 3**). During the entire 4 d period of darkness, the suppression of the increase in total amino acid levels was attenuated in *atg5-1* and *atg10-1* (**Fig. 4B**). The total amino acid levels in *atg2-1* were greater than those in the WT during this period (**Fig. 4B**). These results suggest that vacuolar degradation of soluble proteins, mostly Rubisco, via autophagy is one of the major routes providing free amino acids during the early period of sugar starvation.

Dark-induced increases in specific amino acid levels are compromised in *atg* mutants

To compare the fluctuations in individual amino acid levels during the dark treatment (Supplementary Table S1), we presented the changes as a heat map (**Fig. 4C**), which indicated that the dark-induced increase of total amino acids results mainly

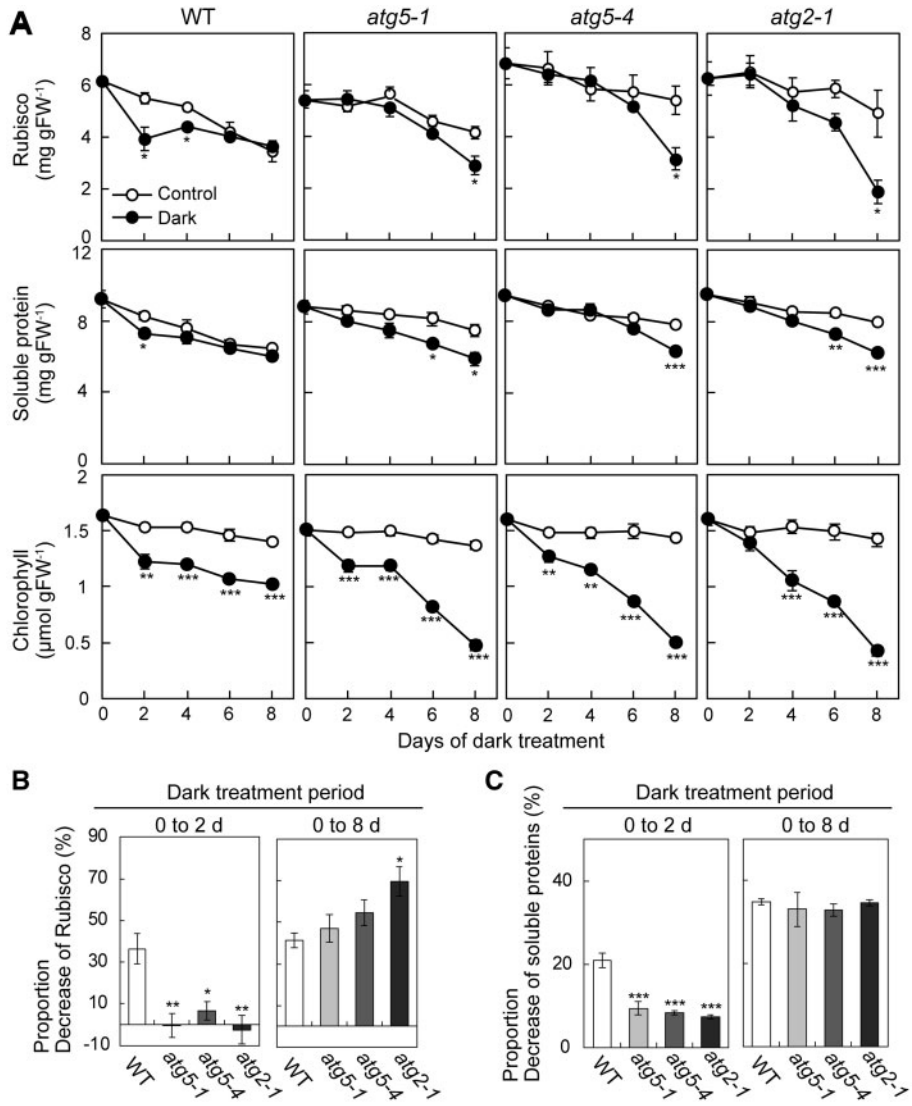

Fig. 3 Effects of impaired autophagy on changes in the levels of Rubisco, soluble protein and Chl during dark treatment. (A) Plants grown for 18 d under long-day conditions were transferred to extended darkness for the indicated number of days. The first to fifth rosette leaves were harvested for analysis. Data are means ± SE (n = 3–4). Asterisks denote significant differences from the control based on a Student's t-test (*$P \leq 0.05$, **$P \leq 0.01$ and ***$P \leq 0.001$). (B and C) Proportional decrease in the amount of Rubisco (B) or soluble proteins (C) in the WT or the *atg* mutants at early (0–2 d) and total (0–8 d) stages of the dark treatment relative to the control conditions. Data are means ± SE (n = 3–4). Asterisks denote significant differences from the WT based on a Dunnett's test (*$P \leq 0.05$, **$P \leq 0.01$ and ***$P \leq 0.001$).

from increases in histidine (His), leucine (Leu), valine (Val), isoleucine (Ile), phenylalanine (Phe), Lys, tyrosine (Tyr), arginine (Arg), asparagine (Asn) and glutamate (Glu). Tryptophan (Trp) was not detected in the control plants but was present in the dark-treated plants (Supplementary Table S1), suggesting that Trp contents also increased during the dark treatment. The data therefore indicate that large increases of basic amino acids (Lys, Arg and His), aromatic amino acids (Phe, Tyr and Trp) and BCAAs (Val, Leu and Ile), as well as Asn and Glu, occur at the early period of sugar starvation. We compared the levels of these amino acids in the WT and *atg* mutants before and after a 2 d dark treatment (**Fig. 5**), and revealed that the increases of the BCAAs, Lys, Tyr and Arg are suppressed in all *atg* mutant lines. These results indicate that these amino acids are released from vacuolar protein degradation via autophagy.

Aspartate (Asp), Asn, glutamine (Gln) and Glu were present at high absolute concentrations in the plants (**Fig. 5**; Supplementary Fig. S4). Among these amino acids, Gln and Asp levels rapidly decreased in the WT and the *atg* mutants after the 2 d dark treatment (Supplementary Fig. S4), while Asn and Glu levels were largely increased (**Fig. 5**). Among these four amino acids, the Glu levels were higher in all *atg* mutants than in the WT before the dark treatment (**Fig. 5**).

Comparison of amino acid composition of Rubisco with free amino acid levels in leaves

Supplementary Fig. S5 shows a comparison of the free amino acid composition before and after the dark treatment. Prior to the dark treatment, Gln, Glu and Asp constituted the majority of free amino acids, representing approximately 70% of the free

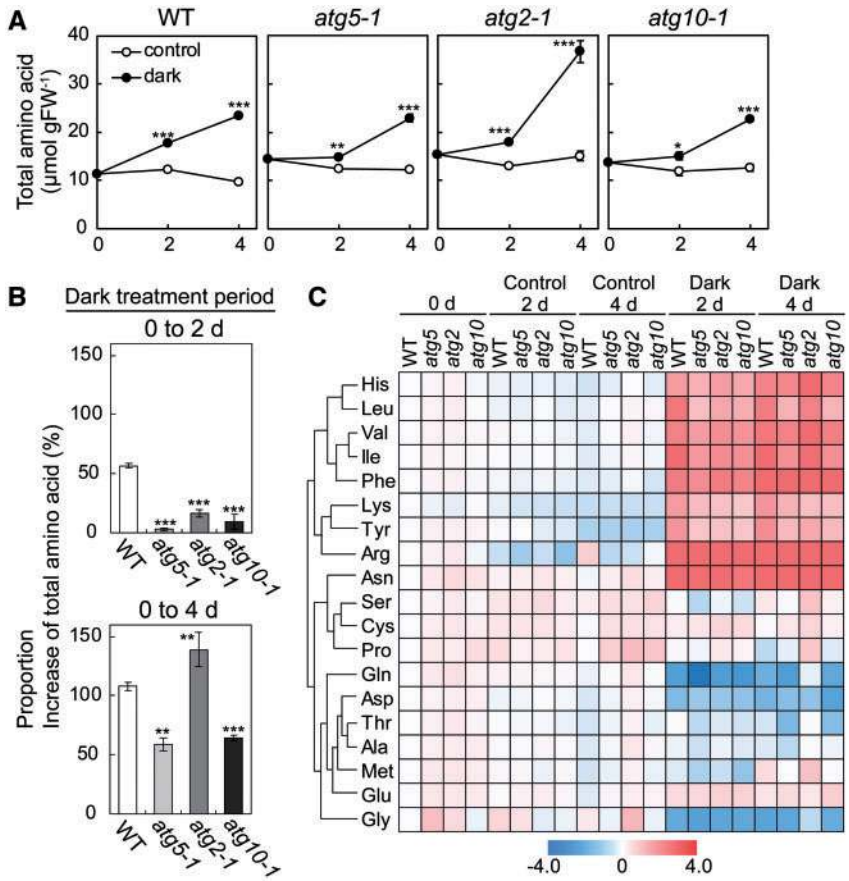

Fig. 4 Impaired autophagy suppresses increases in total amino acid contents during early periods of dark treatment. (A) Changes in total amino acid concentrations in the wild type (WT) and the *atg* mutants under control and dark conditions. Data are means ± SE ($n = 4$). Asterisks denote significant differences from the control based on Student's *t*-test (*$P \leq 0.05$, **$P \leq 0.01$ and ***$P \leq 0.001$). (B) Increases of total amino acid levels in *atg* mutants vs. the WT during a 2 or 4 d dark treatment. Data are means ± SE ($n = 4$). Asterisks denote significant differences from the WT based on Dunnett's test (**$P \leq 0.01$ and ***$P \leq 0.001$). (C) Log_2 values of concentrations of individual amino acids relative to those of the WT in the control condition are represented as a heat map ($n = 4$). The absolute concentrations of individual amino acids at each time point are indicated in Supplementary Table S1.

amino acid pool, while the nine basic amino acids, BCAAs and aromatic amino acids together comprised only 3% of the total free amino acids. After the 2 d dark treatment, the proportion of the basic amino acids, BCAAs and aromatic amino acids increased to 23% of the total free amino acids. Supplementary Fig. S5 also shows the theoretical amino acid composition of Rubisco, which contains 20 types of amino acid, each accounting for 1.5–9.1% of the total amino acids in the protein, with the basic amino acids, BCAAs and aromatic amino acids comprising up to 45% of the amino acid residues in Rubisco. Thus, differences in both the composition and pool sizes of the free amino acids and the Rubisco-bound amino acids may partly explain the drastic increases in the levels of basic amino acids, BCAAs and aromatic amino acids after dark treatment, which causes a concomitant Rubisco degradation.

Relationship between autophagy and amino acid catabolism via the ETF/ETFQO system

Previous studies revealed that BCAAs are catabolized via the IVDH enzyme and the ETF/ETFQO system to provide an alternative energy source during sugar starvation (Ishizaki et al. 2005, Ishizaki et al. 2006, Araújo et al. 2010, Peng et al. 2015). Given that autophagy disruption had a large effect on the dark-induced increases of the BCAAs (**Fig. 5**), we inspected the relationship between autophagy and the IVDH and ETF/ETFQO system. We checked the transcript levels of several genes known to be involved in amino acid catabolism via the ETF/ETFQO system (Supplementary Fig. S6) in the WT, *atg5-1* and the *ivdh-1* and *etfqo-1* mutants. BCAA transaminase 2 (BCAT2) and the branched-chain α-keto acid dehydrogenase complex subunit E1A1 (BCKDH E1A1) are involved in BCAA catabolism by providing substrates to IVDH (Angelovici et al. 2013, Hildebrandt et al. 2015, Peng et al. 2015). The transcript levels of *BCAT2*, *BCKDH E1A1*, *IVDH* and *ETFQO* were found to be increased after the 2 d dark treatment in both the WT and *atg5-1* (Supplementary Fig. S6). We further measured the transcript levels of the nine *ATG8* family members (*AtATG8a*–*AtATGi*) in these plants (Supplementary Fig. S6). ATG8 is a ubiquitin-like protein required for the formation of autophagosomal membranes (Ichimura et al. 2000). The transcript levels of several *ATG8* genes increased after the 2 d dark treatment in the WT and the mutants (Supplementary Fig. S6).

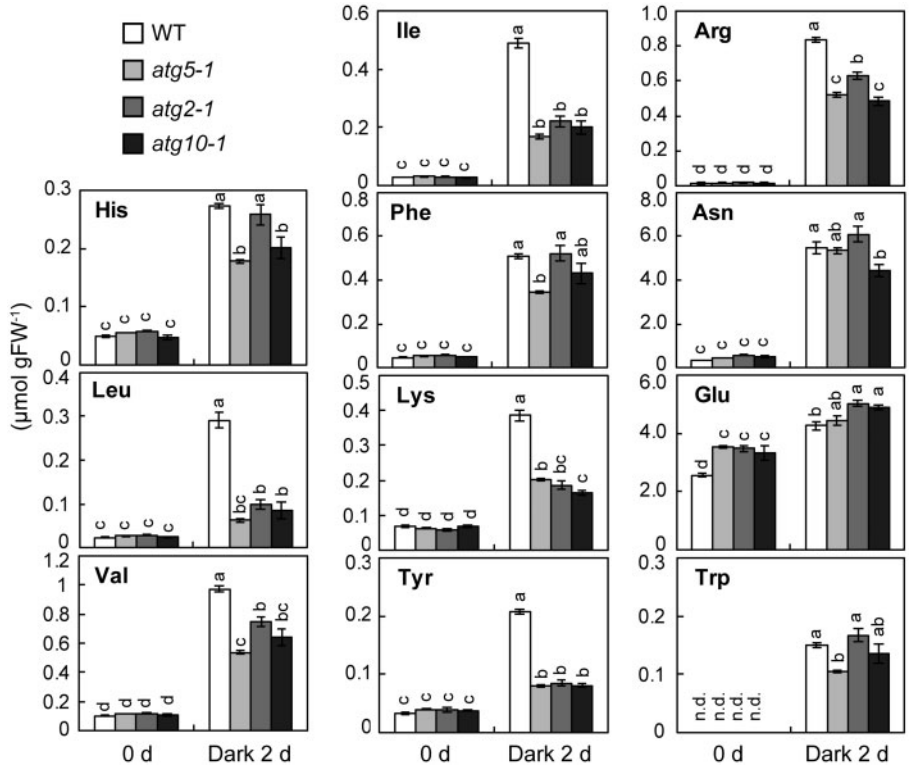

Fig. 5 Increases in the levels of specific amino acids after dark treatment are partially compromised in the *atg* mutants. The absolute concentrations of amino acids that increased during the dark treatment are presented for the wild type (WT) and the *atg* mutants before and after a 2 d dark treatment. Data are means ± SE ($n = 4$). Different letters denote significant differences from each other based on a Tukey test ($P \leq 0.05$). n.d., not detected.

These results further suggested that both autophagy and the BCAA catabolic pathway are activated during the dark treatment.

To examine if the IVDH and ETF/ETFQO system functions from the early stages of sugar starvation, we compared the amino acid levels between *ivdh-1* or *etfqo-1* and the WT (**Figs. 6, 7**). The total amino acid levels increased similarly after the dark treatment among those plants (**Fig. 6A, B**), mainly caused by increases in the BCAAs, basic amino acids, aromatic amino acids and Asn (**Fig. 6C;** Supplementary Table S2). The dark-induced increase of Glu was suppressed in *ivdh-1* and *etfqo-1* (**Fig. 7**). Among the individual amino acids that did not increase in the dark-treated WT (Supplementary Fig. S7), the decrease in alanine (Ala) levels was exacerbated in both *ivdh-1* and *etfqo-1*. These results are consistent with previous findings, which might reflect the attenuation of BCAA catabolism in these mutants (Ishizaki et al. 2005, Araújo et al. 2010). The accumulation of BCAAs after 2 d of dark treatment was enhanced in *ivdh-1* and *etfqo-1* compared with the WT (**Fig. 7**), supporting the suggestion that BCAAs are catabolized via IVDH and the ETF/ETFQO system from an early period of dark treatment.

We next attempted to assess the contribution of autophagy to the BCAA catabolic pathway mediated by IVDH and the ETF/ETFQO system during the early period of sugar starvation. To this end, we produced double mutants impaired in autophagy and amino acid catabolism via the ETF/ETFQO system (*ivdh-1 atg5-1* or *etfqo-1 atg5-1*), and compared their changes in free amino acid levels after a 2 d dark treatment with those of their respective single mutants (**Figs. 6, 7**). The enhanced increases in BCAA levels in *ivdh-1* or *etfqo-1* were countered when these lines were crossed with *atg5-1* (**Fig. 7**). The dark-induced increases in Ile and Leu were reduced in *ivdh-1 atg5-1* to 47.2% and 49.6%, respectively, of that of *ivdh-1*, while in *etfqo-1 atg5-1* their increases were reduced to 54.7% and 58.1%, respectively, of that of *etfqo-1*. These results suggest that autophagy contributes approximately half of the free BCAA supply during the early period of the sugar starvation, which is consistent with the hypothesis that autophagy is one of the main routes for providing BCAAs for catalysis via IVDH and ETFQO in response to sugar starvation.

The *ivdh-1* and *etfqo-1* mutations did not affect the dark-induced increases in the levels of basic amino acids (Lys, Arg and His) and aromatic amino acids (Phe, Tyr and Trp) compared with the WT plants (**Fig. 7**). In the double mutant lines *ivdh-1 atg5-1* and *etfqo-1 atg5-1*, the increases of these six amino acids were suppressed, relative to their respective single mutants, which was similar to the comparison between *atg5-1* and the WT (**Fig. 7**).

Additive effects of the *atg5* and the *ivdh* or *etfqo* mutations on the susceptibility to dark treatment

We attempted to assess the impact of individual amino acid levels in *atg5-1*, *ivdh-1* and *etfqo-1* plants and their double mutants on tolerance to sugar starvation. To compare their

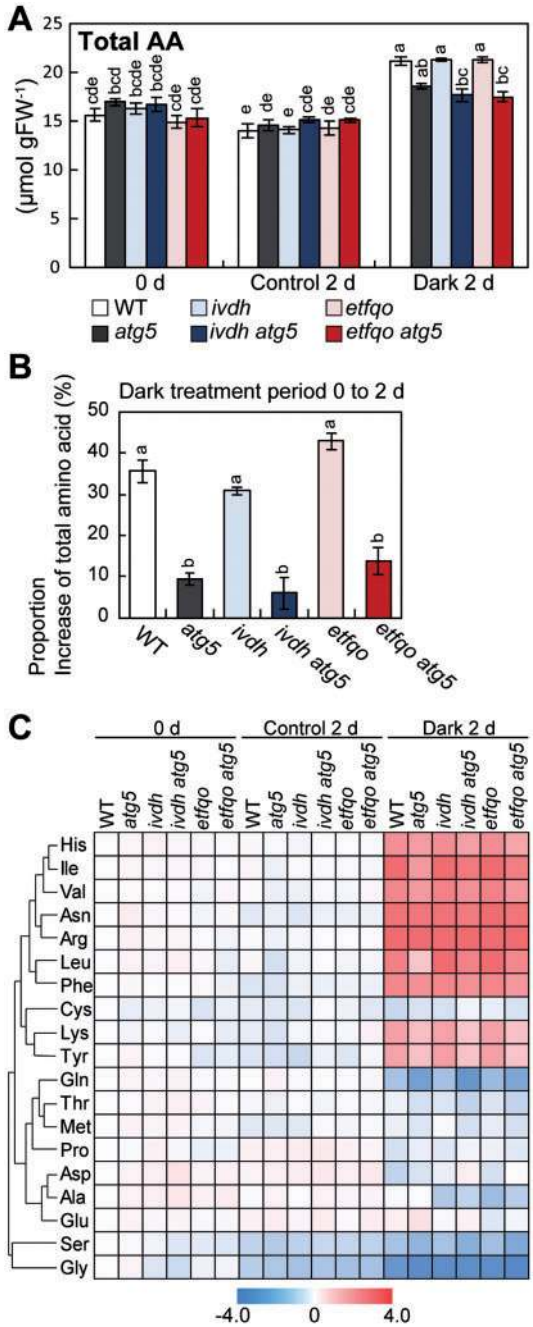

Fig. 6 Changes in amino acid concentrations in *atg5-1*, *ivdh-1*, *etfqo-1* and the double mutants after a 2 d dark treatment. (A) The absolute concentrations of total amino acids are compared among individual genotypes. Data are means ± SE (n = 3). (B) Increases of total amino acid levels during a 2 d dark treatment. Different letters denote significant differences from each other based on a Tukey test ($P \leq 0.05$). (C) Log_2 values of concentrations of individual amino acids relative to those of the wild type (WT) in the control conditions are represented as a heat map (n = 3). The absolute concentrations of individual amino acids at each time point are indicated in Supplementary Table S2.

susceptibility to sugar starvation, we cultured the mutant plants for 18 d under long-day conditions, followed by 0–6 d of darkness (**Fig. 8A**). After the dark treatment, the F_v/F_m ratio (maximum quantum efficiency of PSII photochemistry) was measured as a diagnostic of leaf senescence (Oh et al. 1996). Thereafter, the plants were returned to long-day conditions and grown for 7 d, and the whole-plant phenotypes were observed. F_v/F_m declined more rapidly in the single mutants (*atg5-1*, *ivdh-1* and *etfqo-1*) than in the WT in the dark treatment, and the decline was even faster in the double mutants (*ivdh-1 atg5-1* and *etfqo-1 atg5-1*) than in the single mutants (**Fig. 8B**). WT plants were completely tolerant of dark treatments up to 6 d in duration, as they resumed growth and their shoot tissues remained healthy (**Fig. 8C**). The *atg5-1*, *indh-1* and *etfqo-1* single mutants were more susceptible than the WT; none of these plants survived after the 6 d dark treatment (**Fig. 8B, C**). Both double mutants (*ivdh-1 atg5-1* and *etfqo-1 atg5-1*) were more susceptible to sugar starvation than their respective single mutants; *ivdh-1 atg5-1* failed to recover after the 4 d dark treatment and *etfqo-1 atg5-1* failed to recover from a 3 d treatment (**Fig. 8C**). An increased susceptibility to the dark treatment was also observed in the double mutant of *etfqo-1* with another autophagy-deficient mutant, *atg2-1* (Supplementary Fig. S8).

The *d2hgdh* mutation has a smaller effect than the *ivdh* or *etfqo* mutation on susceptibility to dark treatment

The dark-induced increase of Lys was largely suppressed in the *atg* plants compared with the WT (**Fig. 5**), and previous studies indicated that Lys may be catabolized via a D2HGDH enzyme-related process (Araújo et al. 2010, Engqvist et al. 2014); however, the transcript level of *D2HGDH* was not elevated after 2 d of dark treatment (Supplementary Fig. S6). We examined the dark treatment sensitivity of *d2hgdh1-2* and its double mutants with *atg5-1* or *atg2-1*. Although some of its lower leaves died, *d2hgdh1-2* survived the 6 d dark treatment (Supplementary Figs. S8, S9). Unlike *ivdh-1* and *etfqo-1*, no clear increase in dark treatment sensitivity was observed in the double mutants of *d2hgdh1-2* with *atg2-1* or *atg5-1* (Supplementary Figs. S8, S9). We further monitored changes in the free amino acid levels in *d2hgdh1-2* and the *d2hgdh1-2 atg5-1* double mutant (Supplementary Fig. S10); however, Lys levels were not significantly different between the WT and *d2hgdh1-2* or between *atg5-1* and *d2hgdh1-2 atg5-1* after 2 d of dark treatment.

Discussion

Importance of vacuolar degradation of stromal proteins via autophagy during the early period of sugar starvation

The current study shows that vacuolar protein degradation via autophagy is a major source of free amino acids, especially free BCAAs, for the subsequent catabolic pathways during early stages of sugar starvation in mature leaves. Rubisco is the most abundant soluble protein in leaves (Evans 1989). The degradation of Rubisco was largely suppressed in *atg* mutants during the early stages of the dark treatment (**Figs. 2, 3**). In WT plants, we observed the vacuolar accumulation of RCBs, a type of autophagosome transporting stromal proteins, along

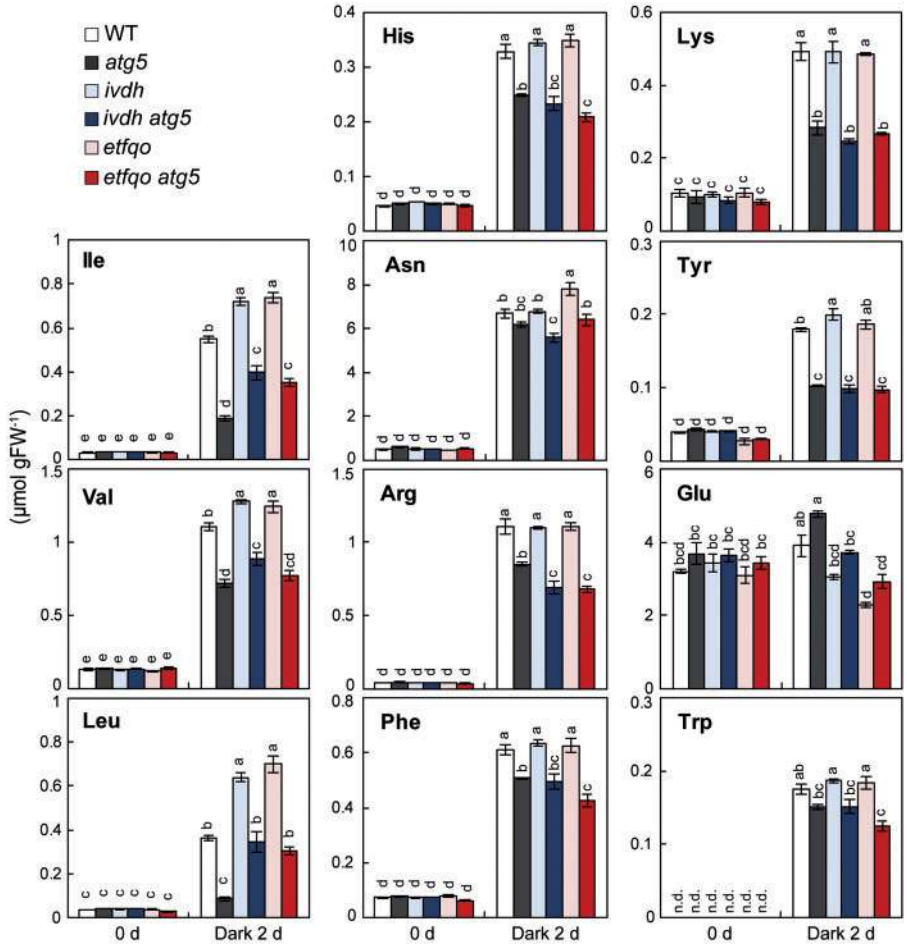

Fig. 7 Increases in amino acid levels in *atg5-1*, *ivdh-1*, *etfqo-1* and the double mutants after a 2 d dark treatment. The absolute concentrations of amino acids that increased during the dark treatment in wild-type plants are shown before and after a 2 d dark treatment. Data are means ± SE (n = 4). Different letters denote significant differences from each other based on a Tukey test ($P \leq 0.05$). n.d., not detected.

with the vacuolar accumulation of free fluorescent proteins, which derive from the vacuolar processing of our Rubisco–fluorescent protein fusion (**Fig. 2**; Supplementary Fig. S2). Our previous studies also identified a distinct type of chloroplast-targeted autophagy that transports entire chloroplasts including the thylakoidal proteins, termed chlorophagy (Wada et al. 2009, Izumi et al. 2017). When chlorophagy is activated, chloroplasts exhibiting a Chl signal accumulate in the vacuolar lumen (Izumi et al. 2017); however, this phenomenon was not observed after 2 d of dark treatment in the present study (**Fig. 2**). In addition, the mitochondria did not appear to degrade after the 2 d dark treatment (Supplementary Fig. S1), which is reasonable since the IVDH and ETF/ETFQO system are localized in mitochondria (Ishizaki et al. 2005, Ishizaki et al. 2006, Araújo et al. 2010). Overall, it is conceivable that Rubisco is the major protein that is degraded during the early period of sugar starvation, and that this degradation is mainly accomplished via RCBs. During extended periods of darkness, Rubisco does not function in CO_2 fixation and is therefore a suitable target for degradation.

In response to an extended (8 d) period of dark treatment, WT plants decreased their levels of Chl, soluble protein and Rubisco during the early stages (0–2 d) of dark treatment but attenuated those decreases during the subsequent period (2–8 d; **Fig. 3**; Supplementary Fig. S3). Indeed, WT plants appear to utilize a 'stand-by mode' to wait for suboptimal environments to improve, repressing their energy consumption after some remodeling of their intracellular proteomes, as previously suggested (Keech et al. 2007). In contrast, the *atg* mutants did not decrease their protein levels as much as the WT during the early period of sugar starvation; instead, they had enhanced decreases in their Chl and protein levels during the subsequent period of treatment (**Fig. 3**; Supplementary Fig. S3). This supports the idea that the *atg* mutants cannot utilize a stand-by mode due to their shortages of amino acids and energy, and must continue to consume cellular components in an autophagy-independent manner. This unfavorable situation would promote necrotic cell death, which also greatly enhances the declines of the leaf Chl and protein levels, and ultimately leads to the early death of the *atg* mutants under dark conditions (**Figs. 3, 8**; Supplementary Figs. S8, S9).

Contrary to previous findings that demonstrated the involvement of autophagy in the vacuolar degradation of starch granules and the massive starch accumulation in several

atg mutants, including *atg5-1* (Wang et al. 2013), we found that the starch degradation in *atg5-1* occurred as usual under dark conditions (**Fig. 1**), which was also the case in our previous study (Izumi et al. 2013). Autophagy appears not to be important for starch degradation in Arabidopsis under our experimental conditions.

The importance of BCAA catabolism during the early period of sugar starvation

This study suggests that autophagy is a major source of free BCAAs during sugar starvation, and that their catabolism is essential for the adaptation of plants to photoassimilate-limited conditions. Catabolic products of free amino acids can ultimately be provided to the TCA cycle for use in mitochondrial ATP synthesis (Hildebrandt et al. 2015). It is estimated that ATP production from BCAA catabolism is relatively higher than when using other individual amino acids (Hildebrandt et al. 2015). In fact, a recent study revealed that Arabidopsis mutants defective in other BCAA catabolism enzymes, including those both upstream and downstream of IVDH, exhibit sensitivity to dark treatment in addition to *ivdh-1* and *etfqo-1* (Peng et al. 2015). This report supports our conclusion that the catabolism of BCAAs released from vacuolar protein degradation via autophagy plays a fundamental role in the adaptation of Arabidopsis to sugar starvation.

Sucrose-non-fermentation1-related protein kinase 1 (SnRK1) is reported to be an energy sensor protein that regulates the global change of gene expression in response to sugar starvation. The transient overexpression of an Arabidopsis SnRK1 gene, *KIN10*, elevated the transcription of some *ATG* and BCAA catabolism genes (Baena-González et al. 2007). A recent study further indicated that both *ATG* and BCAA catabolism genes are up-regulated by a transcription factor protein, Arabidopsis TRANSCRIPTION ACTIVATION FACTOR1 (ATAF1), during sugar starvation (Garapati et al. 2015); therefore, both autophagy and BCAA catabolism may be co-operatively controlled at the transcript level to respond to energy depletion.

Release of free amino acids by protein degradation may explain the drastic increases in specific amino acid levels during sugar starvation

Our results suggest that autophagy of soluble proteins, especially Rubisco, provides free amino acids during the early stages of the dark treatment response (**Fig. 3**). Basic amino acids, BCAAs and aromatic amino acids are present at extremely low concentrations under normal conditions, but their contents drastically increase after dark treatment (**Figs. 4, 5**). Differences in both the composition and pool sizes of the free amino acids and the Rubisco-bound amino acids may partly explain the drastic increases in the levels of those amino acids after dark treatment (Supplementary Fig. S5). A previous study also estimated that pools of free amino acids within a cell are 100- to 1,000-fold smaller than the corresponding pools of protein-bound amino acids (Hildebrandt et al. 2015). Impaired protein degradation due to autophagy deficiency caused the

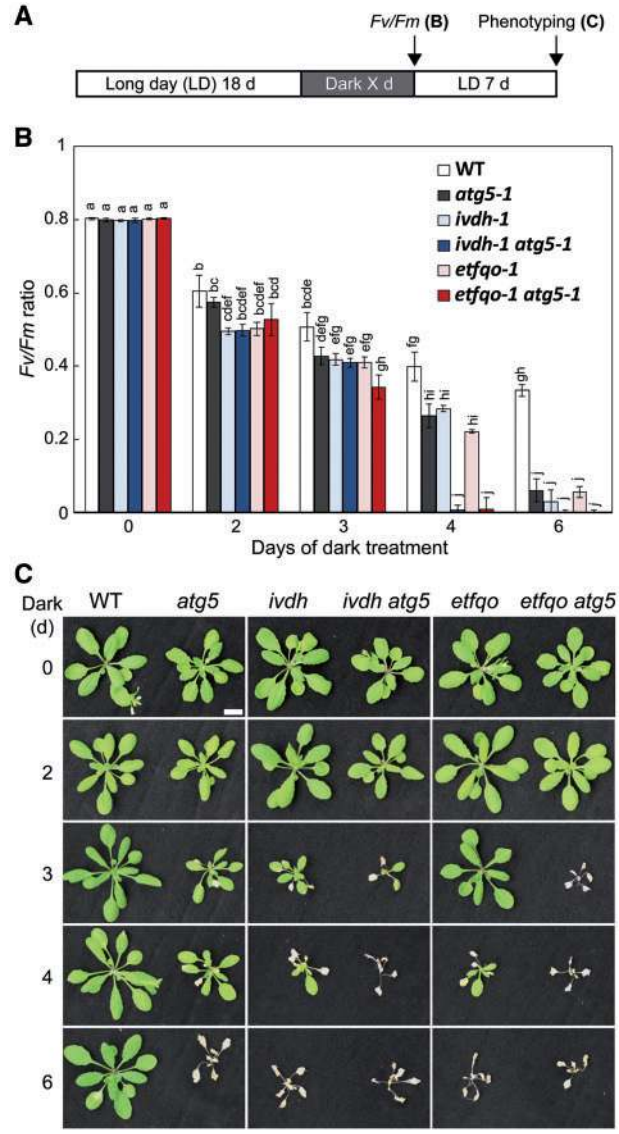

Fig. 8 Increased sensitivity of *atg5-1*, *ivdh-1* and *etfqo-1* to dark treatment is further enhanced in the double mutants. (A) Schematic representation of this experiments. Plants were grown for 18 d under long-day conditions then kept in darkness for the indicated number of days, followed by a 7 d recovery under long-day conditions. (B) The F_v/F_m ratio (maximum quantum efficiency of PSII photochemistry) in leaves was measured just after a dark treatment for the indicated number of days. Data represent means ± SE (n = 5). Different letters denote significant differences from each other based on a Tukey test ($P \leq 0.05$). (C) Photographs of plants after the 7 d recovery following dark treatment for the indicated number of days. Scale bar = 10 mm.

suppression of increases in total amino acid, basic amino acid, BCAA and aromatic amino acid levels during the early period of sugar starvation (**Figs. 3–5**). These results indicate that autophagy plays a major role in supplying these amino acids through the degradation of proteins, primarily Rubisco, following dark treatment

Among Asn, Asp, Gln and Glu, which were present at high absolute concentrations in control plants, Gln and Asp levels rapidly decreased and Asn and Glu levels were greatly increased

during dark treatment regardless of genotypes (Figs. 4, 5; Supplementary Fig. S4). These results are consistent with the previous finding that Gln is converted to Asn by DIN6, because Asn has a higher nitrogen/carbon ratio and is metabolically less valuable (active) than Gln in dark conditions (Lam et al. 1994, Fujiki et al. 2001).

Enhanced sensitivity of the *ivdh atg* and *etfqo atg* double mutants to dark treatment may be linked to the free amino acids available for energy production

In addition to the increases in BCAA levels expected in the *ivdh-1* and *etfqo-1* mutants after the dark treatment, the increases of aromatic and basic amino acids were also found to be suppressed in *ivdh-1 atg5-1* and *etfqo-1 atg5-1* in comparison with the single *ivdh-1* or *etfqo-1* mutants (Fig. 7). This suggests that the catabolism of aromatic and basic amino acids is partially compromised in *ivdh-1 atg5-1* and *etfqo-1 atg5-1*, in addition to their defects in BCAA catabolism. The catabolism of aromatic and basic amino acids may also be an important adaptive response to sugar starvation, because Tyr and Lys are calculated to have a high efficiency for ATP production (Hildebrandt et al. 2015). Our data suggested that *D2HGDH*-related Lys catabolism is not crucial for dark-induced amino acid catabolism (Supplementary Figs. S8–S10). A previous study similarly indicated that IVDH is more important than D2HGDH for the alternative respiration pathway in darkness (Araújo et al. 2010). However, other D2HGDH-independent Lys catabolic pathways were reported (Hildebrandt et al. 2015), and such pathways may be involved in the dark-induced catabolism of Lys.

When the individual amino acid levels of the double mutants *ivdh-1 atg5-1* or *etfqo-1 atg5-1* are compared with those of the *atg5-1* single mutant, their BCAA increases are shown not to be completely compromised (Fig. 7). This suggests that autophagy-independent protein degradation, possibly via the ubiquitin–proteasome system or intrachloroplast proteases, can also supply free BCAAs. The catabolism of BCAAs as a whole is therefore also considered to be compromised in *ivdh-1 atg5-1* and *etfqo-1 atg5-1* in comparison with the *atg5-1* single mutant, in which the use of free amino acids specifically derived from autophagy-dependent protein degradation is compromised. According to these hypotheses, the available free amino acids for ATP production in the *ivdh atg* or *etfqo atg5* double mutants are reduced relative to those in the *atg*, *ivdh* or *etfqo* single mutants, which may explain their enhanced sensitivity to dark treatment (Fig. 8).

Amino acid recycling through vacuolar protein degradation

The present study establishes an important role for the vacuole in the metabolic changes during the adaptation to stress conditions, in which vacuolar protein degradation supplies free amino acids for subsequent catabolic pathways as a plant metabolic strategy to promote fitness under photoassimilate-limited conditions. Energy availability from photosynthesis fluctuates under ever-changing environmental conditions, including stress conditions that perturb the conversion of energy by photosynthesis and respiration (Baena-González and Sheen 2008); therefore, amino acid recycling through vacuolar protein degradation is an important adaptive response for plant survival. This study indicates that a major route that transports proteins, which are the major amino acid reservoirs, into the vacuole is autophagy. To achieve the recycling of amino acids released from lytic protein degradation, the free amino acids must be transported into mitochondria to undergo BCAA catabolism (Araújo et al. 2011); however, the intracellular transport of protein degradation-derived amino acids, including vacuolar membrane-bound amino acid transporters, is poorly understood (Tegeder 2012). This vacuolar transport mechanism must be elucidated to enable our understanding of the overall system of plant amino acid recycling through vacuolar protein degradation.

Materials and Methods

Plant materials, growth conditions and dark treatments

The *Arabidopsis thaliana* ecotype Columbia was used for all experiments. The T-DNA-insertional autophagy-deficient mutants used were *atg5-1* (SAIL_129_B07; Thompson et al. 2005), *atg5-4* (SALK_151148; Ishida et al. 2008), *atg2-1* (SALK_076727; Yoshimoto et al. 2009) and *atg10–1* (SALK_084434; Phillips et al. 2008). The T-DNA-insertional knockout mutants of BCAA or Lys catabolism used were *ivdh-1* (GABI_756_G02; Araújo et al. 2010), *d2hgdh1-2* (SAIL_844_G06; Araújo et al. 2010) and *etfqo-1* (SALK_007870; Ishizaki et al. 2005). All *atg* mutants were kindly provided by Dr. Kohki Yoshimoto, Meiji University. The other mutants, namely *ivdh-1*, *d2hgdh1-2* and *etfqo-1*, were obtained from the Arabidopsis Biological Resource Center. Double mutants were generated by sexual crosses. Homozygous mutants were identified by PCR using primers for specific genes as described in the above references. Transgenic plants in the WT or *atg* mutant backgrounds expressing the *RBCS2B–GFP* or *RBCS2B–RFP* fusion were obtained by sexual crosses, or were previously described (Ishida et al. 2008, Ono et al. 2013). Transgenic plants expressing *GFP* driven by the *DIN6* (At3g47340) promoter, as well as transgenic plants in the WT or *atg5-4* background expressing the mitochondrial *IDH–GFP* fusion, were generated with new constructs as described below.

Arabidopsis plants were sown in a planting mix containing nutrients (Takii) and grown at 23°C in a growth room under a 14/10 h photoperiod provided by fluorescent lamps (100 μmol m^{-2} s^{-1}). Dark treatments of whole plants began at the end of the light period 18 d after sowing. The first to fifth rosette leaves, which had been expanding until 18 d, were harvested, immediately frozen in liquid nitrogen and stored in a deep freezer for subsequent analysis. In each set of experiments, two or three independent biological replicates were carried out with three or four plants; similar results were obtained, and representative results are shown in the figures.

Plasmid construction and plant transformation

For transgenic plants expressing *GFP* driven by the *DIN6* promoter, the *DIN6* promoter region (the 5′ region 624 bp upstream of the start codon) was amplified from Arabidopsis genomic DNA by PCR using primers 5′-CACCTCATTTGAAATGTGTTCAC-3′ and 5′-GTTTTTTTTTTGAAGAAAGTG-3′, then cloned into the pENTR/D/TOPO vector (Thermo Fisher Scientific). The coding region was transferred to the pGWB504 vector (Nakagawa et al. 2007) in an LR recombination reaction, then introduced into Arabidopsis by the floral dip method for *Agrobacterium*-mediated transformation in planta (Clough and Bent 1998). For transgenic plants expressing the mitochondrial *IDH–GFP* fusion, a DNA fragment from the 5′ region 417 bp upstream of the start codon to the region just before the stop codon of *IDH* (At4g35260) was amplified from Arabidopsis genomic DNA by PCR using primers 5′-CACCCTTCTTTCACCAAAGCCTTG-3′ and 5′-GTCTAGTTTTGCAATGACCGCATC-3′, and cloned into the pENTR/D/

TOPO vector. The coding region was transferred to the pGWB504 vector (Nakagawa et al. 2007) in an LR recombination reaction, then introduced into Arabidopsis as described above.

Measurement of carbohydrate levels

Starch, Suc, Glc and Fru levels were measured using an F-kit for α-Glc/Suc/Fru (Roche Diagnostics) and an F-kit for starch (Roche Diagnostics), as previously described (Izumi et al. 2010).

Measurement of Rubisco, soluble protein and Chl levels

Frozen rosette leaves were homogenized in an ice-chilled mortar and pestle in 50 mM HEPES–NaOH buffer (pH 7.5) containing 10% (v/v) glycerol, 0.8% (v/v) 2-mercaptoethanol and a proteinase inhibitor cocktail (complete Mini; Roche). Chl contents were determined as described by Arnon (1949). Soluble protein contents were determined using a Bio-Rad protein assay with bovine serum albumin (BSA; Bio-Rad) as the standard. For the Rubisco determination, Triton X-100 (0.1%, final concentration) was added to the remaining homogenate. After centrifugation, the supernatant was mixed with an equal volume of SDS sample buffer containing 200 mM Tris–HCl (pH 8.5), 2% (w/v) SDS, 5% (v/v) 2-mercaptoethanol and 20% (v/v) glycerol, then boiled for 3 min before being subjected to SDS–PAGE. The Rubisco content was determined spectrophotometrically by formamide extraction of the Coomassie brilliant blue R-250-stained bands corresponding to the large and small subunits of Rubisco, which were separated by SDS–PAGE. Calibration curves were constructed using BSA (Albumin Standard; Thermo Fisher Scientific).

Measurement of free amino acid levels

Free amino acid levels were measured using ultra performance liquid chromatography (UPLC) as previously described (Konishi et al. 2014). Leaves pre-chilled in liquid nitrogen were homogenized (Tissue Lyser II; Qiagen), then mixed with 10 mM HCl and centrifuged at 20,500×*g* for 10 min. The supernatant was filtered through a filter unit (Amicon Ultra-0.5 ml Centrifugal Filters 3K; Merck Millipore), and the flow-through was used as the free amino acid extract. Free amino acids were derivatized using an AccQ-Tag Ultra Derivatization Kit (Waters) according to the manufacturer's instructions. Labeled amino acids were measured with a ACQUITY UPLC H-Class (Waters) using amino acid standard H (Thermo Fisher Scientific) combined with Asn, Gln and Trp as the standard.

Quantitative reverse transcription–PCR (qRT–PCR) analysis

Total RNA was isolated from rosette leaves using the RNeasy kit (Qiagen) and used for cDNA synthesis with the PrimeScript RT Reagent Kit with gDNA Eraser (TAKARA). An aliquot of the synthesized cDNA derived from 20 ng total RNA was subjected to a qRT–PCR analysis with the SYBR FAST qPCR Kit (Kapa Biosystems) using a real-time PCR detection system (CFX96; Bio-Rad). The transcript levels of the respective genes were normalized using the data for 18S rRNA. The sequences of the primers, which were used in previous studies (Rose et al. 2006, Kwon et al. 2010, Izumi et al. 2012, Angelovici et al. 2013, Izumi et al. 2013, Peng et al. 2015), are shown in Supplementary Table S3.

Chl fluorescence measurement

The maximum quantum yield of PSII [$F_v/F_m = (F_m - F_0)/F_m$] was measured with a pulse-modulated fluorometer (Junior-PAM; Walz). After a 20 min dark incubation of each plant, F_0 and subsequently F_m were measured in the third rosette leaves using a measuring light and a saturating pulse.

Image analysis by confocal laser-scanning microscopy

Confocal laser-scanning microscopy (CLSM) was performed with a Nikon C1si system equipped with a CFI Plan Apo VC ×60 water immersion objective (NA = 1.20; Nikon) or a Carl Zeiss LSM 800 system equipped with a C-apochromat LD ×63 water immersion objective (NA = 1.15; Carl Zeiss). The third or fourth rosette leaves were mounted on slides with cover glasses. GFP and Chl were excited with the 488 nm laser, and RFP was excited with a combination of the 488 nm laser and the 543 nm line of a helium–neon laser, or a 561 nm diode laser. Emissions were detected at 500–530 nm for sGFP, 565–615 nm for mRFP and >650 nm for Chl using a multichannel detector with filters. The relative intensity of the vacuolar RFP fluorescence was measured at the same area of the center part of mesophyll cell sections using EZ-C1 imaging software for the C1si system (Nikon) or ZEN2 imaging software for the LSM 800 system (Carl Zeiss).

Rubisco–GFP processing assay

The processing of Rubisco–GFP in the vacuole and the subsequent release of free GFP were detected with a fluorescence imager (LAS-4000 mini; Fujifilm) equipped with a blue light-emitting diode (460 nm EPI) and a band pass filter (510DF10) for GFP following the non-denaturing PAGE as previously described (Ono et al. 2013, Izumi et al. 2015).

Statistical analysis

Statistical analyses in this study and the clustering of individual amino acids in **Fig. 4C** and **Fig. 6C** were performed with JMP software (SAS Institute).

Supplementary Data

Supplementary data are available at PCP online.

Funding

This work was supported by Japan Society for the Promotion of Science and the Ministry of Education, Culture, Sports, Science and Technology, Japan [KAKENHI (grant Nos. 26506001 and 17H05050 to M.I. and 25119703, 26660286 and 15H04626 to H.I.); the GRENE/NC-CARP project (to A.M.)]; Building of Consortia for the Development of Human Resources in Science and Technology [to M.I.]; the Japan Science and Technology Agency (JST) PRESTO [grant No. JPMJPR16Q1 to M.I.]; and the Program for Creation of Interdisciplinary Research [to M.I.] at Frontier Research Institute for Interdisciplinary Sciences, Tohoku University, Japan.

Acknowledgments

We thank Dr. Tomoyuki Yamaya and his lab members, Drs. Noriyuki Konishi, Keiki Ishiyama, Soichi Kojima and Toshihiko Hayakawa, for technical advice regarding amino acid quantification and the use of UPLC. We also thank Drs. Kohki Yoshimoto and Yoshinori Ohsumi for providing the Arabidopsis *atg* mutants, and Dr. Tsuyoshi Nakagawa for providing the pGWB vectors. We appreciate the Arabidopsis Biological Resource Center and original donors for providing the Arabidopsis T-DNA-insertional knockout mutants.

Disclosures

The authors have no conflicts of interest to declare.

References

Angelovici, R., Lipka, A.E., Deason, N., Gonzalez-Jorge, S., Lin, H.N., Cepela, J., et al. (2013) Genome-wide analysis of branched-chain amino acid levels in Arabidopsis seeds. *Plant Cell* 25: 4827–4843.

Araújo, W.L., Tohge, T., Ishizaki, K., Leaver, C.J. and Fernie, A.R. (2011) Protein degradation—an alternative respiratory substrate for stressed plants. *Trends Plant Sci.* 16: 489–498.

Araújo, W.L., Ishizaki, K., Nunes-Nesi, A., Larson, T.R., Tohge, T., Krahnert, I., et al. (2010) Identification of the 2-hydroxyglutarate and isovaleryl-CoA dehydrogenases as alternative electron donors linking lysine catabolism to the electron transport chain of *Arabidopsis* mitochondria. *Plant Cell* 22: 1549–1563.

Arnon, D.I. (1949) Copper enzymes in isolated chloroplasts. Polyphenoloxidase in *Beta vulgaris*. *Plant Physiol.* 24: 1–15.

Avin-Wittenberg, T., Bajdzienko, K., Wittenberg, G., Alseekh, S., Tohge, T., Bock, R., et al. (2015) Global analysis of the role of autophagy in cellular metabolism and energy homeostasis in Arabidopsis seedlings under carbon starvation. *Plant Cell* 27: 306–322.

Baena-González, E., Rolland, F., Thevelein, J.M. and Sheen, J. (2007) A central integrator of transcription networks in plant stress and energy signalling. *Nature* 448: 938–942.

Baena-González, E. and Sheen, J. (2008) Convergent energy and stress signaling. *Trends Plant Sci.* 13: 474–482.

Clough, S.J. and Bent, A.F. (1998) Floral dip: a simplified method for *Agrobacterium*-mediated transformation of *Arabidopsis thaliana*. *Plant J.* 16: 735–743.

Engqvist, M.K.M., Esser, C., Maier, A., Lercher, M.J. and Maurino, V.G. (2014) Mitochondrial 2-hydroxyglutarate metabolism. *Mitochondrion* 19: 275–281.

Evans, J.R. (1989) Photosynthesis and nitrogen relationships in leaves of C_3 plants. *Oecologia* 78: 9–19.

Fujiki, Y., Yoshikawa, Y., Sato, T., Inada, N., Ito, M., Nishida, I., et al. (2001) Dark-inducible genes from *Arabidopsis thaliana* are associated with leaf senescence and repressed by sugars. *Physiol. Plant.* 111: 345–352.

Garapati, P., Feil, R., Lunn, J.E., Van Dijck, P., Balazadeh, S. and Mueller-Roeber, B. (2015) Transcription factor Arabidopsis Activating Factor1 integrates carbon starvation responses with trehalose metabolism. *Plant Physiol.* 169: 379–390.

Graf, A., Schlereth, A., Stitt, M. and Smith, A.M. (2010) Circadian control of carbohydrate availability for growth in *Arabidopsis* plants at night. *Proc. Natl. Acad. Sci. USA* 107: 9458–9463.

Hanaoka, H., Noda, T., Shirano, Y., Kato, T., Hayashi, H., Shibata, D., et al. (2002) Leaf senescence and starvation-induced chlorosis are accelerated by the disruption of an Arabidopsis autophagy gene. *Plant Physiol.* 129: 1181–1193.

Hildebrandt, T.M., Nesi, A.N., Araujo, W.L. and Braun, H.P. (2015) Amino acid catabolism in plants. *Mol. Plant* 8: 1563–1579.

Ichimura, Y., Kirisako, T., Takao, T., Satomi, Y., Shimonishi, Y., Ishihara, N., et al. (2000) A ubiquitin-like system mediates protein lipidation. *Nature* 408: 488–492.

Ishida, H., Izumi, M., Wada, S. and Makino, A. (2014) Roles of autophagy in chloroplast recycling. *Biochim. Biophys. Acta* 1837: 512–521.

Ishida, H., Yoshimoto, K., Izumi, M., Reisen, D., Yano, Y., Makino, A., et al. (2008) Mobilization of rubisco and stroma-localized fluorescent proteins of chloroplasts to the vacuole by an *ATG* gene-dependent autophagic process. *Plant Physiol.* 148: 142–155.

Ishizaki, K., Larson, T.R., Schauer, N., Fernie, A.R., Graham, I.A. and Leaver, C.J. (2005) The critical role of *Arabidopsis* electron-transfer flavoprotein:ubiquinone oxidoreductase during dark-induced starvation. *Plant Cell* 17: 2587–2600.

Ishizaki, K., Schauer, N., Larson, T.R., Graham, I.A., Fernie, A.R. and Leaver, C.J. (2006) The mitochondrial electron transfer flavoprotein complex is essential for survival of Arabidopsis in extended darkness. *Plant J.* 47: 751–760.

Izumi, M., Wada, S., Makino, A. and Ishida, H. (2010) The autophagic degradation of chloroplasts via rubisco-containing bodies is specifically linked to leaf carbon status but not nitrogen status in Arabidopsis. *Plant Physiol.* 154: 1196–1209.

Izumi, M., Hidema, J., Makino, A. and Ishida, H. (2013) Autophagy contributes to nighttime energy availability for growth in Arabidopsis. *Plant Physiol.* 161: 1682–1693.

Izumi, M., Ishida, H., Nakamura, S. and Hidema, J. (2017) Entire photodamaged chloroplasts are transported to the central vacuole by autophagy. *Plant Cell* 29: 377–394.

Izumi, M., Tsunoda, H., Suzuki, Y., Makino, A. and Ishida, H. (2012) *RBCS1A* and *RBCS3B*, two major members within the *Arabidopsis RBCS* multigene family, function to yield sufficient Rubisco content for leaf photosynthetic capacity. *J. Exp. Bot.* 63: 2159–2170.

Izumi, M., Hidema, J., Wada, S., Kondo, E., Kurusu, T., Kuchitsu, K., et al. (2015) Establishment of monitoring methods for autophagy in rice reveals autophagic recycling of chloroplasts and root plastids during energy limitation. *Plant Physiol.* 167: 1307–1320.

Keech, O., Pesquet, E., Ahad, A., Askne, A., Nordvall, D., Vodnala, S.M., et al. (2007) The different fates of mitochondria and chloroplasts during dark-induced senescence in *Arabidopsis* leaves. *Plant Cell Environ.* 30: 1523–1534.

Konishi, N., Ishiyama, K., Matsuoka, K., Maru, I., Hayakawa, T., Yamaya, T., et al. (2014) NADH-dependent glutamate synthase plays a crucial role in assimilating ammonium in the Arabidopsis root. *Physiol. Plant.* 152: 138–151.

Kwon, S.I., Cho, H.J., Jung, J.H., Yoshimoto, K., Shirasu, K. and Park, O.K. (2010) The Rab GTPase RabG3b functions in autophagy and contributes to tracheary element differentiation in Arabidopsis. *Plant J.* 64: 151–164.

Lam, H.M., Peng, S.S.Y. and Coruzzi, G.M. (1994) Metabolic regulation of the gene encoding glutamine-dependent asparagine synthetase in *Arabidopsis thaliana*. *Plant Physiol.* 106: 1347–1357.

Liu, Y.M. and Bassham, D.C. (2012) Autophagy: pathways for self-eating in plant cells. *Annu. Rev. Plant Biol.* 63: 215–237.

Makino, A., Sato, T., Nakano, H. and Mae, T. (1997) Leaf photosynthesis, plant growth and nitrogen allocation in rice under different irradiances. *Planta* 203: 390–398.

Matile, P. (1987) The sap of plant cells. *New Phytol.* 105: 1–26.

Muntz, K. (2007) Protein dynamics and proteolysis in plant vacuoles. *J. Exp. Bot.* 58: 2391–2407.

Nakagawa, T., Suzuki, T., Murata, S., Nakamura, S., Hino, T., Maeo, K., et al. (2007) Improved Gateway binary vectors: high-performance vectors for creation of fusion constructs in transgenic analysis of plants. *Biosci. Biotechnol. Biochem.* 71: 2095–2100.

Nakatogawa, H., Suzuki, K., Kamada, Y. and Ohsumi, Y. (2009) Dynamics and diversity in autophagy mechanisms: lessons from yeast. *Nat. Rev. Mol. Cell Biol.* 10: 458–467.

Oh, S.A., Lee, S.Y., Chung, I.K., Lee, C.H. and Nam, H.G. (1996) A senescence-associated gene of *Arabidopsis thaliana* is distinctively regulated during natural and artificially induced leaf senescence. *Plant Mol. Biol.* 30: 739–754.

Ono, Y., Wada, S., Izumi, M., Makino, A. and Ishida, H. (2013) Evidence for contribution of autophagy to rubisco degradation during leaf senescence in *Arabidopsis thaliana*. *Plant Cell Environ.* 36: 1147–1159.

Peng, C., Uygun, S., Shiu, S.H. and Last, R.L. (2015) The impact of the branched-chain ketoacid dehydrogenase complex on amino acid homeostasis in Arabidopsis. *Plant Physiol.* 169: 1807–1820.

Phillips, A.R., Suttangkakul, A. and Vierstra, R.D. (2008) The ATG12-conjugating enzyme ATG10 is essential for autophagic vesicle formation in *Arabidopsis thaliana*. *Genetics* 178: 1339–1353.

Rose, T.L., Bonneau, L., Der, C., Marty-Mazars, D. and Marty, F. (2006) Starvation-induced expression of autophagy-related genes in Arabidopsis. *Biol. Cell* 98: 53–67.

Schertl, P. and Braun, H.P. (2014) Respiratory electron transfer pathways in plant mitochondria. *Front. Plant. Sci* 5: 163.

Soudry, E., Ulitzur, S. and Gepstein, S. (2005) Accumulation and remobilization of amino acids during senescence of detached and attached

leaves: in planta analysis of tryptophan levels by recombinant luminescent bacteria. *J. Exp. Bot.* 56: 695–702.

Tegeder, M. (2012) Transporters for amino acids in plant cells: some functions and many unknowns. *Curr. Opin. Plant Biol.* 15: 315–321.

Thompson, A.R., Doelling, J.H., Suttangkakul, A. and Vierstra, R.D. (2005) Autophagic nutrient recycling in Arabidopsis directed by the ATG8 and ATG12 conjugation pathways. *Plant Physiol.* 138: 2097–2110.

Tsukada, M. and Ohsumi, Y. (1993) Isolation and characterization of autophagy-defective mutants of *Saccharomyces cerevisiae*. *FEBS Lett.* 333: 169–174.

Wada, S., Ishida, H., Izumi, M., Yoshimoto, K., Ohsumi, Y., Mae, T., et al. (2009) Autophagy plays a role in chloroplast degradation during senescence in individually darkened leaves. *Plant Physiol.* 149: 885–893.

Wang, Y., Yu, B., Zhao, J., Guo, J., Li, Y., Han, S., et al. (2013) Autophagy contributes to leaf starch degradation. *Plant Cell* 25: 1383–1399.

Yao, Z.Y., Delorme-Axford, E., Backues, S.K. and Klionsky, D.J. (2015) Atg41/Icy2 regulates autophagosome formation. *Autophagy* 11: 2288–2299.

Yoshimoto, K. (2012) Beginning to understand autophagy, an intracellular self-degradation system in plants. *Plant Cell Physiol.* 53: 1355–1365.

Yoshimoto, K., Jikumaru, Y., Kamiya, Y., Kusano, M., Consonni, C., Panstruga, R., et al. (2009) Autophagy negatively regulates cell death by controlling NPR1-dependent salicylic acid signaling during senescence and the innate immune response in *Arabidopsis*. *Plant Cell* 21: 2914–2927.